Journal of Materials Chemistry B

Accepted Manuscript

ROYAL SOCIETY OF CHEMISTRY

www.rsc.org/materialsB

Journal of Materials Chemistry B

RSCPublishing

ARTICLE

Impact of confining 3-D polymer networks on dynamics of bacterial ingress and self-organisation

Vi Khanh Truong, David E. Mainwaring,* Pandiyan Murugaraj, Khuong Duy Nguyen, and Elena P. Ivanova*

Corresponding authors: demainwaring@swin.edu.au ; eivanova@swin.edu.au

Cite this: DOI: 10.1039/x0xx00000x

Received 00th January 2015,
Accepted 00th January 2015

DOI: 10.1039/x0xx00000x

www.rsc.org/

Studies of microbial interactions during motility, micro-structuring and colonisation have predominately been limited to surface associated bacteria involving materials such as semi-solid biomolecular hydrogels and thin liquid films. Recently, these surfaces have been extended to synthetic polymers where they provide defined chemistries and structural properties. However, precise details of microbial ingress into the confined fluid volume of synthetic 3-D hydrogel networks and their subsequent microstructuring remain to be defined. Here, we show that Gram-positive and Gram-negative bacteria internally populate mesoporous polyacrylate hydrogels by quantifying: the dynamic advancing population front and the resultant spontaneous self-organisation into well-defined clusters and micro-colonies. Polymer chain conjugated fluorescent nanoparticles indicated that both bacterial clusters and micro-colonies associated directly with the polymer chains of the mesoporous hydrogel. Protonation of the K-polyacrylate made chains more hydrophobic and globular in conformation, reducing the swelling of the hydrogel by half. However, the bacterial population increased by 30% indicating the dominance of hydrophobic and viscoelastic interactions as well as the cation chemistry within the confined fluids of synthetic polymer hydrogels despite pore size reductions of 50%. Synthetic polymer hydrogels having a range of porosities when swollen together with controllable chemical and structural functionality can potentially offer well-defined microenvironments for bacterial populations in advancing biotechnologies such as inoculants and substrates in the production of therapeutic agents.

1. Introduction

Polymeric hydrogels such as poly(acrylic acid) have been widely used in a number of applications, including the biomedical coatings, soil moisture agents, cell encapsulants and inoculants.[1-3] In particular, the interactions between microbes and hydrogel can lead to advantageous or disadvantageous outcomes in such applications. To date, the interactions between bacteria and materials have focussed (a) in free liquid phases,[4] (b) on the hydrous surfaces of semi-solid hydrogels (e.g. agar),[5,6] and (c) in thin liquid films on solid biomaterials.[7,8] It has been widely recognised that the microenvironment can influence bacterial motility and viability.[9,10] Two of the principal movements associated with surface fluids are swimming and swarming, whereas swimming is an individual endeavour, collective swarming arises from movement of a group of bacteria as widely seen among flagellated bacteria.[11] This suggests that these modes of bacterial surface translocation may also play an important role in optimal foraging strategies, colonisation and population dynamics generally.

Synthetic polymer surfaces have been recognised as providing defined chemical functionality and structural stiffness as well as a uniformity not available with conventional polysaccharide gels such as agar.[12] With little exception, studies of the bacterial physicochemical interactions occurring during motility and population have been limited to surface associated bacteria due to the dominance of surface colonisation within the biosphere.[5] Tuson and Weibel have recently reviewed in detail the bacteria-surface interactions known to govern surface attachment and motility; showing their importance to the resultant physiology and behaviour.[13] Microbial interaction with substrates involves the interplay of long range physical forces followed by specific shorter range biomolecular adhesions. Importantly, of the non-specific physical interactions, entropic hydrophobic interactions usually dominate in aqueous microbial systems.[14-16]

Two important aspects of bacteria - soft matter interactions are gaining research prominence. Biophysical studies define bacteria as self-propelled entities capable of modulating their microenvironments through physical viscosity reductions and superdiffusivity.[9,17,18] Secondly chemical species may alter the

microenvironment itself through exopolymeric molecules (exudates).[18-20] Additionally, bacteria may alter the material structure of their swimming environments by simple pH chnage, significantly increasing the translocation of pathogenic bacteria, *e.g., Helicobacter pylori* reducing the crosslinking of mucosal hydrogel coatings.[21] With contamination of surgically implanted materials becoming a universal challenge and the growing technological interest in microbial encapsulation, the quantification of bacterial dynamics and structuring within well controlled three dimensional microenvironments offered by synthetic polymers underpins further our understandings of the complexity of these interrelationships.

However, the influence of the synthetic three-dimensional (3-D) hydrogel network and its confined fluid phase on microbial behaviour still remains to be detailed. In this study, we investigated how a 3-D polyelectrolyte network of poly(acrylic acid) influences the ingress and self-organized microstructures of *Bacillus subtilis* and *Pseudomonas fluorescens*, to understand the relation between the physical characteristics (microstructures, polymeric charges and hydrophobicity) and microbial behaviour (transport and self-organisation). Here, we recognise that the interface between free liquid and hydrogel substrate has a finite volume with different interactions occurring compared to either the external liquid or the bulk internal hydrous gel, and characterise it as an interphase region. We also show that this polymer hydrogel is inherently heterogeneous with a cellular microstructure even in the fully hydrated state, where the hydrophobicity of the polymer network modulates the spatial distribution of microbes through the dominance of the physicochemical forces that control their approach and adhesion.

2. Experimental details

2.1 Materials

Acrylic acid (AA, anhydrous 99%) containing 180 – 200 ppm of monomethyl ether hydroquinone as inhibitor, methylene bisacrylamide (MBA, 99%) and ammonium persulphate (APS, 98%) and poly(ethylene glycol) (PEG, 35 kDa) were purchased from Sigma Aldrich (Castle Hill, NSW, Australia). Polyacrylic acids were prepared according to Supplementary Information S2.1. Nutrient broth and agar were purchased from Oxoid (Basingstoke, Hampshire, UK) and prepared according to S2.3.

2.2 Hydrogel properties

Hydrogel samples, prepared *in situ* on a Cryo-SEM slit sample holder were frozen with liquid nitrogen and transferred to the Gatan Alto 2500 pre-chamber and cooled to -170°C. The surface of the sample was then fractured in various locations using a scalpel to produce free-break surfaces before sublimation ~20 min at −85 °C. Pt sputter coating followed for 2 min prior to transfer to the microscope cryo-stage (−130 °C) for imaging. Samples were imaged with a FEI NOVA nanoSEM field emission (FEI Company, Hillsboro, Oregon) using the through-the-lens or Everhart-Thornley detector at 5kV accelerating voltage and a working distance of 5mm at different magnifications.

PEG-surfactant stabilised fluorescent nanoparticles (diameter ~10 nm) were prepared and incorporated during syntheses of K-PAA as detailed in S2.2 and used to identify the porous cellular microstructure and define the outer surface of the hydrogel during confocal laser scanning microscopy. The swelling measurements of K-PAA were carried out in MilliQ water according to Horkay, et al.[22] and reported in terms of the swelling ratio Q = swollen mass / initial dry PAA mass. Subsequently deswelling of the hydrogels was quantified by contact with aqueous solutions of 35 kDa poly(ethylene glycol) of known osmotic pressure[22,23] through a semipermeable membrane of cut-off 12.0 kDa.

Viscoelastic measurements of hydrogels were performed with a stress controlled rheometer (DSR 200, Rheometrics, Paulsboro NJ) using vane geometry (vane dimensions: length 20 mm; diameter 20 mm; cup diameter 32 mm and volume about 45 ml) at a constant sample temperature of 25 °C.[24,25] Samples were protected with an environmental chamber under saturated humidity conditions, minimising evaporation from the gel both during swelling and measurement processes. Hydrogels were swollen within the rheometer sample cup with vane in position to allow gel to swell (Q = 100, 200, 300) without disruption at vane surfaces prior to application of external stress. Response of the hydrogels to applied oscillatory stresses (frequency 1 rad/s) in the range of 0.185 to 600 Pa was measured and the viscoelastic parameters extracted.

2.3 Bacterial strains and growth conditions

Bacillus subtilis ATCC 6051^T and *Pseudomonas fluorescens* ATCC 13525 were obtained from the American Type Culture Collection (ATCC, USA). *B. subtilis* and *P. fluorescens* were shown to be facultative aerobic and strictly aerobic, respectively. Bacterial stocks were prepared in 20% glycerol nutrient broth (Oxoid) and stored at −80 °C. Prior to each experiment, bacterial cultures were refreshed from stocks on nutrient agar (Oxoid), and a fresh bacterial suspension was prepared for each of the strains grown overnight in 100 mL of nutrient broth (in 0.5 L Erlenmeyer flasks) at 37 °C for *B. subtilis* and 30 °C for *P. fluorescens* with shaking (120 rpm). Bacterial cells were collected at the logarithmic stage of growth. To ensure that the samples possessed similar numbers of cells despite variations in cell densities among the different strains used, the cell density of each strain was adjusted to OD_{600} = 0.3.

Prior to incubation, hydrogels were swollen to equilibrium in MilliQ water (H_2O) and nutrient broth (NB). Incubation of the bacterial cultures was carried out with pre-swollen K-PAA and H-PAA hydrogels placed within 20 mL of bacterial suspension of OD_{600} = 0.3 and allowed to incubate for 18 and 48 h at 25 °C. After incubation, the samples were gently removed with a mild rinsing step to avoid the disruption on

bacterial colonisation in hydrogels. All experiments were carried out independently in triplicate.

2.4 Visualisation and quantification of bacterial ingress

Freeze-fracture scanning electron microscopy was used to probe *P. fluorescens* ingress and colony formation to depths of ~4 mm depth within the hydrogel network after 72 hours incubation (Fig. S2†). However, to identify and quantify the degree of bacterial colonisation inside hydrogel at various hydrated states, confocal laser scanning microscopy (CLSM) was used to visualise the proportions of live cells and dead cells using LIVE/DEAD BacLight® Bacterial Viability Kit, L7012 as detailed in S2.4. Bacterial suspensions were stained according to the manufacturer's protocol, and imaged using a Fluoview FV10i inverted microscope (Olympus, Tokyo, Japan). For distance measurements of bacterial ingress, three-dimensional stacks were re-sliced using Fluoview® FV 7.0 (Olympus v.1.45b) into the vertical planes (X–Z) and integrated fluorescence intensity of both viable and non-viable cells was calculated along z-axis. Also, to validate the staining - washing procedure of the bacteria-colonised hydrogels, bacteria pre-stained with Syto® 10 (Invitrogen) were shown to give comparable intensities to the post-colonised samples as given in Fig. S1†.

The computer software COMSTAT on the Matlab® platform was used to quantify image stacks of confocal data through a pixel counting method.[26] Four typical confocal image stacks of a particular bacterial strain for each condition was exported into a stack of grey-scale 8-bit images by Fluorview® FV 7.0. Two quantitative parameters of biomass density were used to describe the degree of bacterial ingress into hydrogel: (i) the biovolume representing the overall volume of the biofilm per unit area of substrate, and (ii) percentage coverage of bacteria per unit area. The distance between two bacteria was measured using ImageJ® at 10 locations elected to obtain statistical values.

3. Results and discussion

3.1 Hydrogel characterisation

The material characteristics of swollen polyacrylate (K-PAA) hydrogel are given in Fig. 1 Cryo-scanning electron microscopy (Fig. 1a) showed that the hydrogel formed a cellular structure characteristic of mesoporous hydrogels[27] where ice crystals tend to maintain cell sizes in the range from 40 μm to 100 μm. The evolution of the equilibrium swelling ratio (Q) of the K-PAA together with the hydrogen exchanged form (H-PAA) is given in Fig 1b,c, where it can be seen that removal of the osmotic free energy contribution of the K^+ counterion (Π_{ion})[22] leads to a reduction in swelling (Q) by ~50%. Swelling of the K-PAA hydrogel systematically reduced the micromechanical properties as shown by the changes in storage and viscous moduli K_M (Fig.1d). As swelling is reduced to about half, the strength of the hydrogel (G") reaches a plateau while its elasticity continues to increase (G' > G"). Subsequent de-swelling under imposed osmotic stresses reduced *Q* of the K-PAA to about 33% when the osmotic pressure was -37 kPa (Fig. 1e).

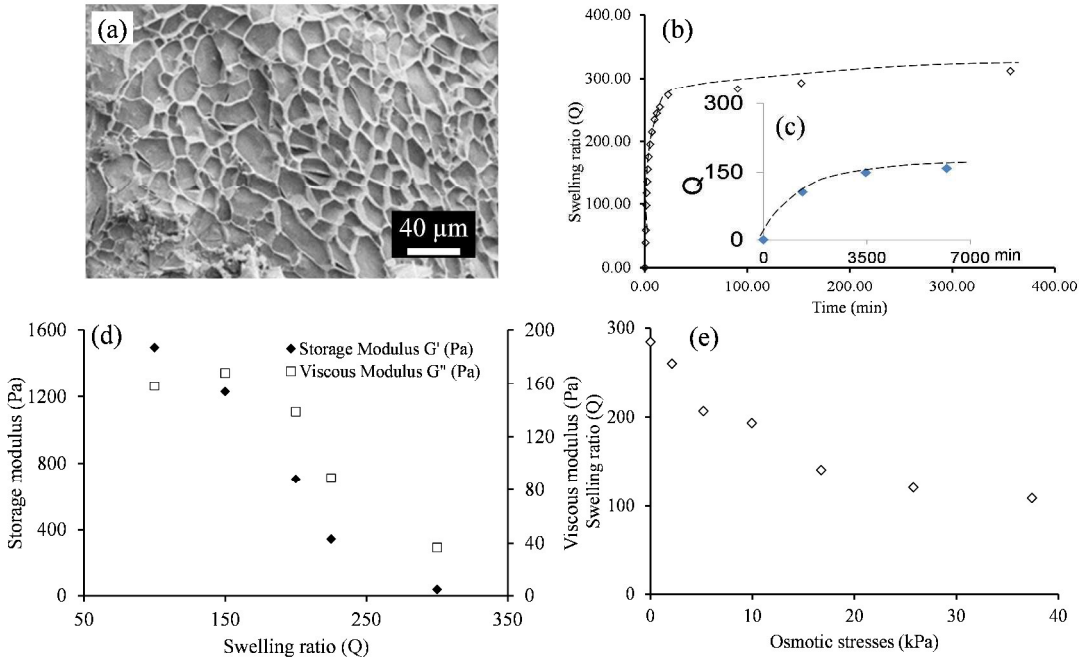

Fig. 1 Potassium polyacrylate hydrogel characteristics: (a) Cryo-SEM image of swollen hydrogel; swelling ratios (*Q*) of (b) K-PAA and (c) H-PAA; (d) viscoelastic properties (storage and viscous moduli K_M) of K-PAA at swelling ratios (Q); and (e) K-PAA deswelling under imposed osmotic stresses.

3.2 Defining the interphase region of swollen hydrogels

With the extensive studies of bacterial motility, adhesion and colonisation on hydrated surfaces,[6,7,13,28,29] quantitative details of the translocation within the confined fluids of polymeric hydrogel networks are still required. To address the complexity of these hydrogel environment quantitatively, the interface between the external and internal regions of the hydrogel was identified precisely by incorporation of fluorescent Ru(dpp) nanoparticles during gel synthesis (Fig. 2). However, fluorescence intensity of silica nanoparticles was found to progressively decrease at larger depths, due to the light scattering behaviour of silica nanoparticles.[30]

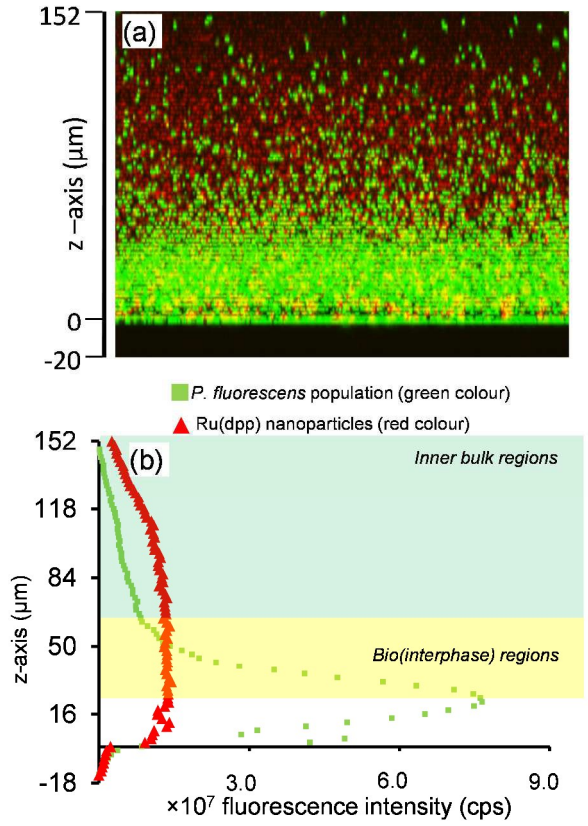

Fig. 2 Defining bio(interphase) and inner bulk regions of bacteria-colonised hydrogel. (a) Cross-section of CLSM image visualising bacterial ingress into K-PAA (green indicates for viable bacteria stained with Syto® 9, and red indicates conjugated fluorescent silica nanoparticles containing Ru(dpp) dyes); (b) fluorescence intensity profile of bacteria and Ru(dpp) nanoparticles defining the surface of hydrogel at z = 0 µm. A clear change in gradient of bacterial population profile represents the end of interphase region; the remaining region of bacterial population defined as the inner bulk region.

Since in approaching an interface, material properties change continuously, *i.e.* there is a 3-D dimensional aspect to the boundary which can be identified as an interphase region followed the inner bulk region of the polymer hydrogel. CLSM imaging (Fig. 2a) clearly indicated that bacteria were able to internally populate the synthetic polymer hydrogel after 18 h which is seen extending to the instrumental limit of ~200 µm. This was subsequently confirmed by lyophilised SEM visualizing bacteria at the centre of a 4 mm hydrogel particle after 4 days (Fig. S2†). Fluorescent intensity profiles (Fig. 2b) identified the hydrogel surface as a distinct discontinuity in nanoparticle fluorescent intensity. The boundary of the (bio) interphase region and commencement of the inner bulk region was distinguished by a clear change in the bacterial population gradient (inflection point) as shown by stained live bacterial fluorescence. Quantification of the bacterial populations was performed by placing $z = 0$ at the hydrogel surface while counting commenced at the maximum fluorescent intensity (z = 22 µm) within interphase region (Fig. 2b), since reductions in bacterial numbers in regions of low z arise from the experimental procedure involved in the necessary washing stages of the staining process prior to CSLM.

3.3 Dynamics of bacterial transport into hydrogels

Two bacteria (*B. subtilis* and *P. fluorescens*) were employed to study ingress into the K-PAA polymeric network, pre-swollen under two nutrient conditions (water and nutrient broth NB). CLSM images and the respective quantitative profiles demonstrate that both bacteria primarily commenced colonising the interphase regions within the 18 hour incubation (Fig. 3, 4 and 5).

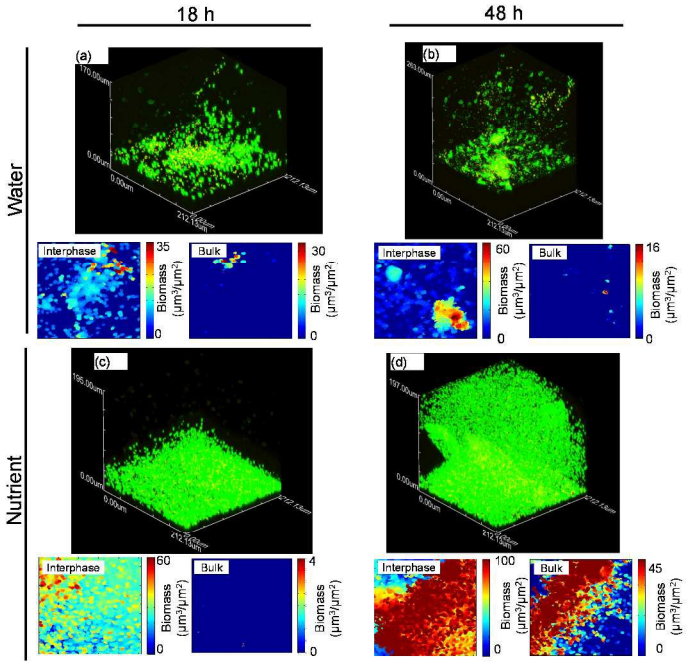

Fig. 3 Ingress of *Bacillus subtilis* into K-PAA hydrogel swollen with: (a, b) water and (c, d) nutrient broth (NB). CLSM images determined by fluorescence intensity showing regions of ingress of bacteria into hydrogel after (a, c) 18 h and (b, d) 48 h incubation, with the corresponding volumetric biomass distributions determined by pixel counting at (bio)interphase and inner bulk regions of the swollen hydrogel over scanning areas of 212 µm × 212 µm.

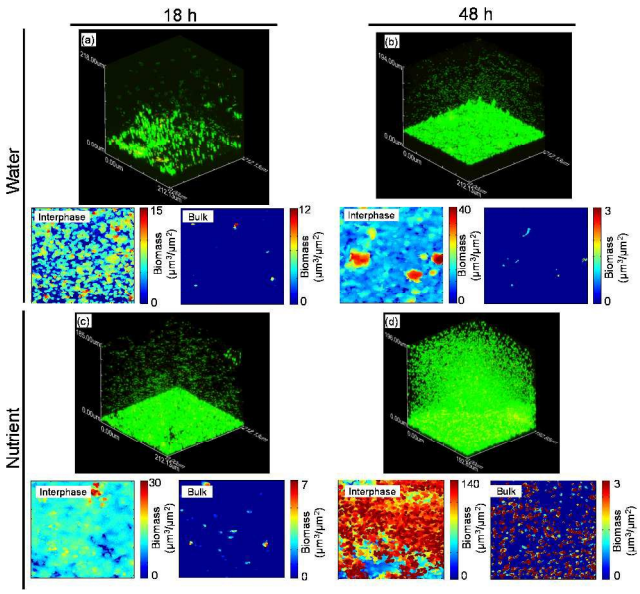

Fig. 4 Ingress of *P. fluorescens* into K-PAA swollen with (a, b) water and (c, d) nutrient broth (NB). CLSM images (fluorescence intensity) showing regions of ingress of bacteria into hydrogel after (a, c) 18 h and (b, d) 48 h incubation, corresponding to Fig. 3.

Gram-negative and motile *P. fluorescens* was observed to colonise ~90% of interphase area after 48 hours incubation. However, Gram-positive *B. subtilis* colonised only 45% of interphase area after 48 hour incubation. In particular, both of *B. subtilis* and *P. fluorescens* were found to significantly ingress into hydrogel pre-swollen with nutrient broth (NB) (Fig. 5).

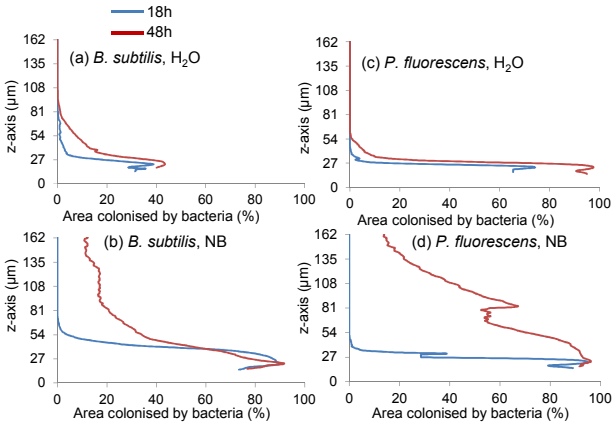

Fig. 5 Population profile of (a, b) *B. subtilis* and (c, d) *P. fluorescens* inside K-PAA after 18 and 48 h. Ingress of bacteria into hydrogel when swollen with (a, c) H_2O and (b, d) nutrient broth (NB) corresponding to Figs. 3 and 4.

3.4 Microbial microstructure within three-dimensional network

Motile bacteria on hydrated surfaces develop well studied diverse patterns that range from periodic rings to dendritic structures characteristic of the collective behaviour of the various genera.[6,7,13,28,29,31] Surface translocation and colony formation is influenced by the degree of hydration,[28] flagella, EPS and bio-surfactants production as well as specific chemotaxis.[5] Bacteria were found to be self-organised locally to form intricate structures within the inner bulk regions of the 3-D polymeric network of K-PAA (Fig. 6a and b) when in the absence of initial nutrient (aqueous gel).

Here, *B. subtilis* was found to consistently form oval micro-colonies inside the network under these stress conditions of poor nutrient. The diameter of these micro-colonies was found to be ~15 μm which contained 10 – 15 bacteria separated by ~150 nm. These microstructures are consistent with *Pseudomonas aeruginosa* clusters observed by Caldara et al. in cystic fibrosis mucus which were 20 μm^2 aggregates consisting of also 10 – 15 cells.[17] While in nutrient rich-conditions (nutrient gel), both of *B. subtilis* and *P. fluoresens* formed chain-like assemblies (Fig. 6c and d) which again had bacteria separation distances of ~150 nm, consistent with the separation gaps in *Proteus mirabilis* linear chains seen in a viscoelastic liquid forming lyotropic liquid crystals.[9] The origin of the repulsive interaction providing these separations was suggested as originating from steric and electrostatic interactions between cells due to the presence of lipopolysaccharide on outer bacterial membranes.

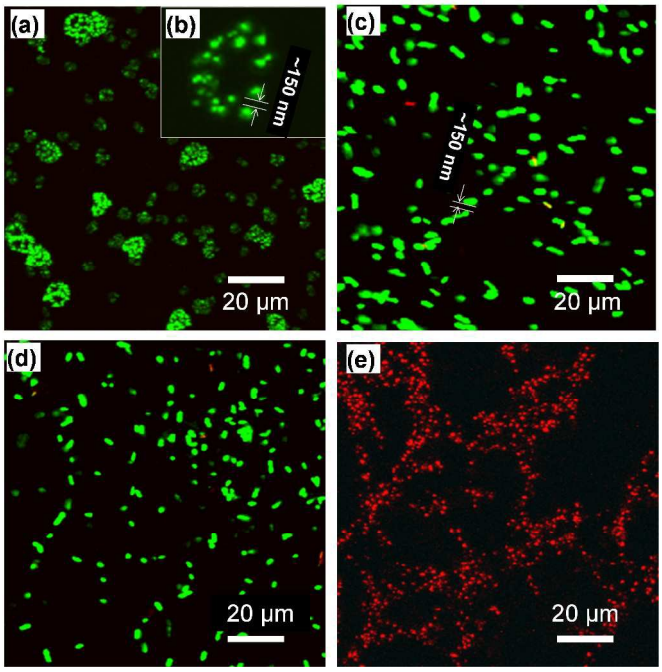

Fig. 6 Microstructure formation within the inner bulk region (a, b) *B. subtilis* forming the micro-colonies in the absence of nutrient; (c) *B. subtilis* and (d) *P. fluorescens* forming chains when nutrient within hydrogels. Microbial aggregates adhering to hydrogel polymer macropores (cell walls) as visualised by (e) fluorescent nanoparticles conjugated to polymer chains.

The formation of PAA polymer chain assemblies (micro-pore walls), similar to those seen in the cryo-SEM (Fig. 1), was confirmed by using the fluorescent nanoparticles conjugated to the PAA chain, which is indicative of the polymer

microstructure continuing in the fully swollen state. Notably, both the bacterial micro-colonies and chain structures shown in Fig. 6 are directly associated with this hydrated polymer microstructure producing patterns of depleted areas having dimensions in a similar range to Fig. 1 (40 –100 μm). These observations are consistent with adherent forms of bacteria often dominating their unattached counterparts.[32]

3.5 Impact of polymer chain charge and hydrophobicity on bacterial ingress

The ingress of *P. fluorescens* into K-PAA and the hydrogen exchanged H-PAA hydrogels is compared in Fig. 7a and b. As noted, removal of the K^+ cation results in a reduction to the hydrated volume (Q) by ~50% resulting the pore size reduced to 20 μm. However, the ingress of the bacterial population, particularly in the inner bulk region, is significantly greater. The respective population distributions (in z) are quantified in Fig. 7b where it is shown that chain neutralisation increases the bacterial transport and the inner population by about 30%.

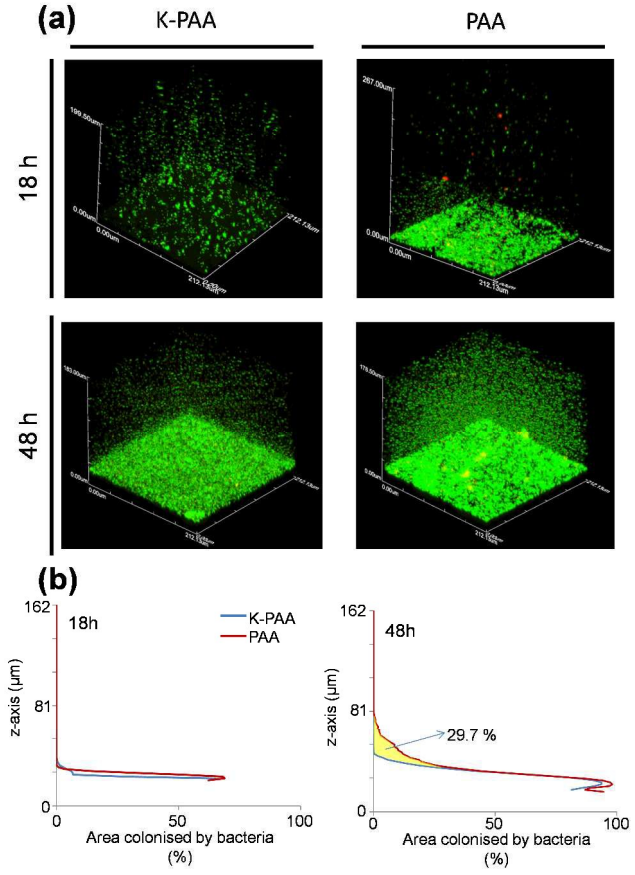

Fig. 7 (a) Ingress of *P. fluorescens* into K-PAA and PAA preswollen in water, shown by CLSM fluorescence imaging after 18 h and 48 h incubation. (b) Quantitative population profile of *P. fluorescens* in K-PAA and PAA at equilibrium swelling *Q* of 300 and 150 respectively after 18 and 48 h. Yellow-highlighted area in (b) represents an increase of 29.7% in bacterial population upon H^+ exchange for K^+.

Polyelectrolyte neutralisation results in the polymer chains becoming more hydrophobic through the entropic driving force reducing the swelling ratio.[22] In doing so, cell wall forming chains are conformationally collapsed[33] while also lowering the influence of the electrical double layer towards negatively charged bacteria such as *P. fluorescens* and *B. subtilis*.[34,35] The additional hydrophobicity of the polymer cell walls increases bacterial cluster formation and ingress, consistent with planar substratum hydrophobicity significantly influencing bacterial adhesion rather than the relative hydrophobicity of the bacterial membrane itself.[36] It has been shown that the moduli of PDMS surfaces, for example, are an important material parameter that directly influences the attachment and stress tolerance of bacterial communities.[37] The concomitant additional stiffness of the protonated PAA chains, as indicated by the modulus $K_M(Q)$ relationship, further enhances microbial ingress and colonisation *albeit* at lower water contents and reductions in pore sizes from 40 μm to 20 μm.

4. Conclusions

In this paper, we clearly demonstrate that Gram-positive *B. subtilis* and Gram-negative *P. fluorescens* were able to internally populate synthetic polyacrylate hydrogels through a dynamic advancing population front together and spontaneous structuring within the confined fluid of the polymer gel. Freeze-fracture SEM identified significant bacteria numbers at the centre of a 4 mm hydrogel particle after 4 days. At shorter times, CSLM quantified the spatial distribution of bacteria (ingress) in the fully hydrated state after identifying the external interface with polymer-conjugated fluorescent nanoparticles recognising the 3-D aspect of the boundary interphase region. In absence of nutrient, *B. subtilis* formed distinctive oval micro-colonies with diameters of ~15 μm and containing 10 – 15 bacteria separated by ~150 nm. However, with nutrient present within gel, both of bacteria assembled into the chain-like structures, with the 150 nm separation distance remaining. Notably, both 3-D micro-colonies and chain structures clearly associated with the mesoporous hydrogel structure as shown by florescent nanoparticle imaging and indicative of the influences of the material properties on self-organisational interactions in biological gels and fluids.[9,38]

Protonation of the K-polyacrylate both reduces chain hydration, making polymer chains more globular and hydrophobic, and reducing the equilibrium swelling but importantly increasing the bacterial population by 30% despite the lower Q although still well within the mobile bulk water regime.[39] It has been shown that bacterial interactions may be readily described by extending the conventional DLVO approach to include shorter range interactions. Also, bacterial immobilization from the free (planktonic) state, a necessary precursor for populating materials, is significantly enhanced by a hydrophobic interaction component resulting from the substrate (polymer chain),[16] rather than bacterial cell hydrophobicity.[14] Additionally, the increased modulus K_M of the protonated PAA hydrogel walls at equilibrium swelling also enhances bacterial adhesion and cluster formation during ingress of the population front consistent with the planar polymer surfaces. This is in contrast to the free swimming state,

where deformable interfaces have been shown to enhance the advancement of single bacteria (soft swimming).[40]

Hence, quantification of the populating dynamics and respective micro-colony structures indicates the dominance of hydrophobic and viscoelastic interactions as well as the cation chemistry[41] within the confined fluids of synthetic polymer hydrogels. By controlling the micro-, meso- and macroporosity, synthetic polymer hydrogels with their controllable chemical and structural functionality have the potential to offer well-defined microenvironments for bacterial populations in advancing biotechnologies such as inoculants and substrates in the production of therapeutic agents.

Acknowledgements

We thank the Commonwealth Cooperative Research Centre for Polymers for their support of the program on microbial aspects of hydrogel materials. We would like to thank A/Prof. Peta Clode and Dr. Jeremy Bougoure for the cryo-SEM image and facilities at the Australian Microscopy and Microanalysis Research Facility at the Centre for Microscopy, Characterisation and Analysis (University of Western Australia).

Notes and references

School of Science, Faculty of Science, Engineering and Technology, Swinburne University of Technology, Hawthorn 3122, Australia

*Corresponding author

Prof. David E. Mainwaring

Faculty of Science, Engineering and Technology, Swinburne University of Technology, email: demainwaring@swin.edu.au.

Elena P. Ivanova

Faculty of Science, Engineering and Technology, Swinburne University of Technology, email: eivanova@swin.edu.au.

† Electronic Supplementary Information (ESI) available. See DOI: 10.1039/b000000x/

1. H. Kamata, X. Li, U. i. Chung and T. Sakai, *Adv. Healthc. Mater.*, 2015.
2. F. Puoci, F. Iemma, U. G. Spizzirri, G. Cirillo, M. Curcio and N. Picci, *Am. J. Agric. Biol. Sci.*, 2008, **3**, 299-314.
3. B. Franz, S. S. Balkundi, C. Dahl, Y. M. Lvov and A. Prange, *Macromol. Biosci.*, 2010, **10**, 164-172.
4. H. C. Berg and L. Turner, *Nature*, 1979, **278**, 349-351.
5. D. B. Kearns, *Nat. Rev. Microbiol.*, 2010, **8**, 634-644.
6. M. F. Copeland and D. B. Weibel, *Soft Matter*, 2009, **5**, 1174-1187.
7. R. M. Harshey, *Annual Review of Microbiology*, 2003, **57**, 249-273.
8. E. Lauga, W. R. DiLuzio, G. M. Whitesides and H. A. Stone, *Biophys. J.*, 2006, **90**, 400-412.
9. P. C. Mushenheim, R. R. Trivedi, H. H. Tuson, D. B. Weibel and N. L. Abbott, *Soft Matter*, 2014, **10**, 88-95.
10. D. E. Fontes, A. L. Mills, G. M. Hornberger and J. S. Herman, *Appl. Environ. Microbiol.*, 1991, **57**, 2473-2481.
11. V. Sourjik and J. P. Armitage, *EMBO J.*, 2010, **29**, 2724-2733.
12. H. H. Tuson, L. D. Renner and D. B. Weibel, *Chem. Commun.*, 2012, **48**, 1595-1597.
13. H. H. Tuson and D. B. Weibel, *Soft Matter*, 2013, **9**, 4368-4380.
14. N. Cerca, G. B. Pier, M. Vilanova, R. Oliveira and J. Azeredo, *Res. Microbiol.*, 2005, **156**, 506-514.
15. P. Teixeira and R. Oliveira, *J Adhes Sci Technol*, 1999, **13**, 1287-1294.
16. Y. L. Ong, A. Razatos, G. Georgiou and M. M. Sharma, *Langmuir*, 1999, **15**, 2719-2725.
17. M. Caldara, R. S. Friedlander, N. L. Kavanaugh, J. Aizenberg, K. R. Foster and K. Ribbeck, *Curr. Biol.*, 2012, **22**, 2325-2330.
18. A. Sokolov and I. S. Aranson, *Phys Rev Lett*, 2009, **103**.
19. A. Be'er and R. M. Harshey, *Biophys. J.*, 2011, **101**, 1017-1024.
20. J. Chen, X. Zhao and A. H. Sayed, in *44th Asilomar Conference on Signals, Systems and Computers, Asilomar 2010*, Pacific Grove, CA, 2010, pp. 1930-1934.
21. J. P. Celli, B. S. Turner, N. H. Afdhal, S. Keates, I. Ghiran, C. P. Kelly, R. H. Ewoldt, G. H. McKinley, P. So, S. Erramilli and R. Bansil, *PNAS*, 2009, **106**, 14321-14326.
22. F. Horkay, I. Tasaki and P. J. Basser, *Biomacromolecules*, 2000, **1**, 84-90.
23. H. Vink, *Eur Polym J*, 1971, **7**, 1411-1419.
24. H. A. Barnes, *J. Non-Newton. Fluid Mech.*, 1995, **56**, 221-251.
25. H. A. Barnes and Q. D. Nguyen, *J. Non-Newton. Fluid Mech.*, 2001, **98**, 1-14.
26. A. Heydorn, A. T. Nielsen, M. Hentzer, C. Sternberg, M. Givskov, B. K. Ersboll and S. Molin, *Microbiology*, 2000, **146**, 2395-2407.
27. I. N. Savina, V. M. Gun'Ko, V. V. Turov, M. Dainiak, G. J. Phillips, I. Y. Galaev and S. V. Mikhalovsky, *Soft Matter*, 2011, **7**, 4276-4283.
28. R. M. Harshey, *Molecular Microbiology*, 1994, **13**, 389-394.
29. E. Lauga and T. R. Powers, *Rep. Prog. Phys.*, 2009, **72**.
30. J. Yun, W. Wang, S. M. Kim, T. S. Bae, S. Lee, D. Kim, G. H. Lee, H. S. Lee and M. Song, *Energy Environ. Sci.*, 2015, **8**, 932-940.
31. J. D. Partridge and R. M. Harshey, *Journal of Bacteriology*, 2013, **195**, 909-918.
32. N. I. Abu-Lail and T. A. Camesano, *Environ. Sci. Technol.*, 2003, **37**, 2173-2183.
33. J. E. Elliott, M. MacDonald, J. Nie and C. N. Bowman, *Polymer*, 2004, **45**, 1503-1510.
34. G. Harkes, J. Feijen and J. Dankert, *Biomaterials*, 1991, **12**, 853-860.
35. A. T. Poortinga, R. Bos, W. Norde and H. J. Busscher, *Surf Sci Rep*, 2002, **47**, 1-32.
36. G. M. Bruinsma, H. C. Van Der Mei and H. J. Busscher, *Biomaterials*, 2001, **22**, 3217-3224.
37. F. Song and D. Ren, *Langmuir*, 2014, **30**, 10354-10362.
38. A. D. Rey, *Soft Matter*, 2010, **6**, 3402-3429.
39. B. Li, L. Xu, Q. Wu, T. Chen, P. Sun, Q. Jin, D. Ding, X. Wang, G. Xue and A. C. Shi, *Macromolecules*, 2007, **40**, 5776-5786.
40. R. Trouilloud, T. S. Yu, A. E. Hosoi and E. Lauga, *Phys Rev Lett*, 2008, **101**.
41. F. Gaboriaud, M. L. Gee, R. Strugnell and J. F. L. Duval, *Langmuir*, 2008, **24**, 10988-10995.

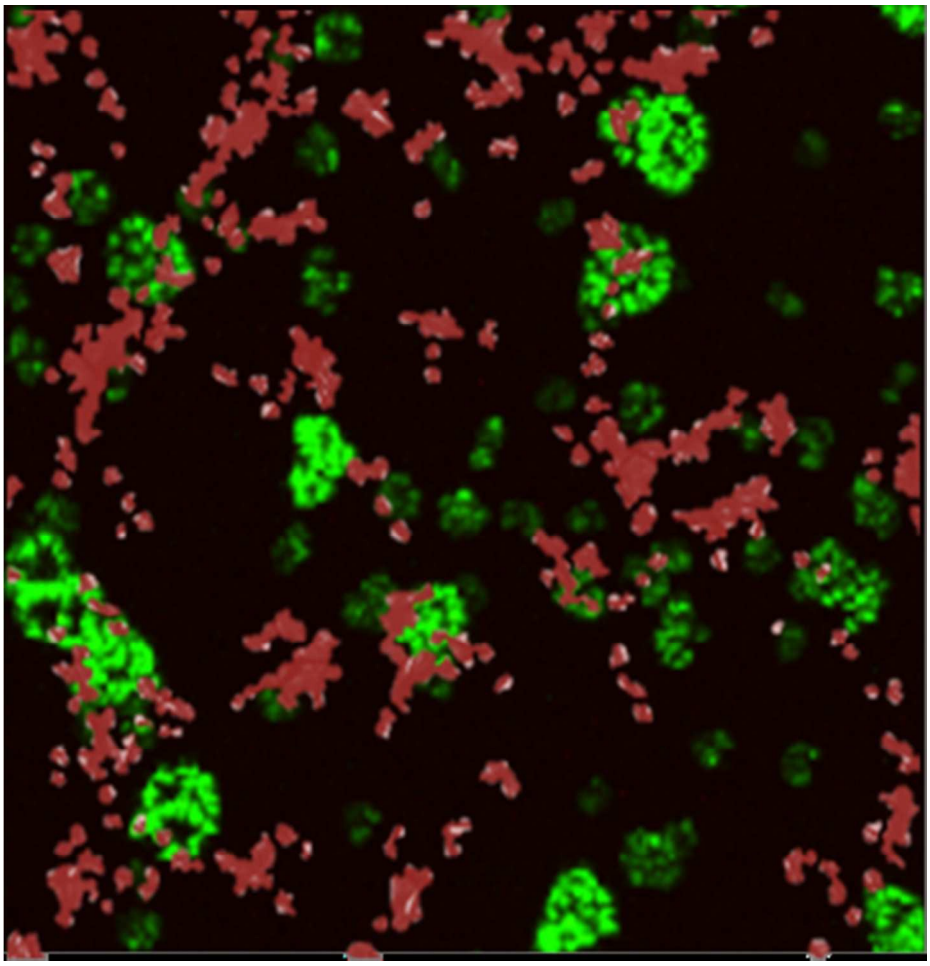

Alignment of microbial colonies along with polymeric cell wall
78x80mm (150 x 150 DPI)